




Article

An Improved Cleaning Protocol for Foraminiferal Calcite from Unconsolidated Core Sediments: HyPerCal—A New Practice for Micropaleontological and Paleoclimatic Proxies

Stergios D. Zarkogiannis ^{1,2,*} , George Kontakiotis ² , Georgia Gkaniatsa ²,
Venkata S. C. Kuppli ^{3,4}, Shashidhara Marathe ³, Kazimir Wanelik ³, Vasiliki Lianou ²,
Evangelia Besiou ², Panayiota Makri ² and Assimina Antonarakou ² 

¹ Department of Earth Sciences, University of Oxford, Oxford OX1 3AN, UK

² Department of Historical Geology-Paleontology, Faculty of Geology & Geoenvironment, School of Earth Sciences, National & Kapodistrian University of Athens, 157 84 Athens, Greece; gkontak@geol.uoa.gr (G.K.); gorgiagkan@gmail.com (G.G.); vlianou@geol.uoa.gr (V.L.); www.eua@hotmail.com (E.B.); pmakri@geol.uoa.gr (P.M.); aantona@geol.uoa.gr (A.A.)

³ Diamond Light Source, Harwell Science and Innovation Campus, Oxford OX11 0DE, UK; charan.kuppli@lightsource.ca (V.S.C.K.); shashidhara.marathe@diamond.ac.uk (S.M.); kaz.wanelik@diamond.ac.uk (K.W.)

⁴ Canadian Light Source, Spectromicroscopy (SM) Beamline, Saskatoon, SK S7N 2V3, Canada

* Correspondence: stergiosz@geol.uoa.gr

Received: 11 November 2020; Accepted: 1 December 2020; Published: 7 December 2020



Abstract: Paleoclimatic and paleoceanographic studies routinely rely on the usage of foraminiferal calcite through faunal, morphometric and physico-chemical proxies. The application of such proxies presupposes the extraction and cleaning of these biomineralized components from ocean sediments in the most efficient way, a process which is often labor intensive and time consuming. In this respect, in this study we performed a systematic experiment for planktonic foraminiferal specimen cleaning using different chemical treatments and evaluated the resulting data of a Late Quaternary gravity core sample from the Aegean Sea. All cleaning procedures adopted here were made on the basis of their minimum potential bias upon foraminiferal proxies, such as the faunal assemblages, degree of fragmentation, stable isotope composition ($\delta^{18}\text{O}$ and $\delta^{13}\text{C}$) and/or Mg/Ca ratios that are frequently used as proxies for surface-ocean climate parameters (e.g., sea surface temperature, sea surface salinity). Six different protocols were tested, involving washing, sieving, and chemical treatment of the samples with hydrogen peroxide and/or sodium hexametaphosphate (Calgon®). Single species foraminifera shell weighing was combined with high-resolution scanning electron microscopy (SEM) and synchrotron X-ray microtomography (μCT) of the material processed by each of the cleaning protocols, in order to assess the decontamination degree of specimen's ultrastructure and interior. It appeared that a good compromise between time and cleaning efficiency is the simultaneous treatment of samples with a mixed hydrogen peroxide and Calgon solution, while the most effective way to almost completely decontaminate the calcareous components from undesirable sedimentary material is a two-step treatment—initially with hydrogen peroxide and subsequently with Calgon solutions.

Keywords: cleaning protocol; unconsolidated core sediments; shell weight; climate reconstruction; synchrotron X-ray microtomography (μCT); foraminiferal-based proxies

1. Introduction

Foraminifera shells (tests) are widely used in paleoceanographic and paleoclimatic studies as biostratigraphic or ecological indicators and through physicochemical analyses as proxies of past oceanic conditions [1]. The tests of different foraminifera species can provide environmental information by means of both physical and chemical analyses. Despite the main focus for environmental reconstructions based on stable isotope [2,3] and trace metal geochemistry [4–6] of foraminifera tests a wealth of information can be attained by their physical analyses that include the study of shell fragmentation [7], abundancies for ecological [8] or biostratigraphic purposes [9] and shell biometry [10–12] including size [13,14] and weight [15,16].

A necessary preliminary step for the use of foraminifera tests in paleoenvironmental studies is the isolation of the test specimens from the muddy sedimentary matrices, that consists of several components. A number of methodologies have been employed to transform the bulk sediment samples into useable micropaleontological material [17,18] as a first level treatment. Although the additional cleaning protocols to isolate primary calcite for geochemical analyses are advanced and several cleaning experiments have sought to quantify the effects of each of these methods on measured elements [19–22], there are only a few studies that assess the efficiency of different treatment procedures on the physical properties of the foraminifera shells such as their weight [21,23].

Studies that focus on foraminifera shell weight measurements are particularly vulnerable to the degree of test contamination, due to their foraminous nature, these specimens have the potential to include contaminants (i.e., sedimentary residuals), which can alter or skew the record toward heavier values [24]. Residual clays or nano-ooze in poral spaces and shell surface obstruct the study of test ultrastructure that yield information about the degree of carbonate dissolution [25] or test porosity [26]. Furthermore, such coatings or infillings (in apertures) often precludes automated recognition software, which is based on morphological features of foraminifera shells [27], from classifying their images correctly [28] and greatly complicate specimen segmentation when using high resolution X-ray tomographic techniques [29]. In the present study, by using light microscope imaging, SEM and X-ray tomography to assess the cleanliness of tests treated with reagents that are established not to alter the fossil geochemical signal, we propose a methodology that effectively diminishes surface and internal specimen contamination.

2. Materials and Methods

For the cleaning test, *Globigerinoides ruber albus* (NCBI:txid2606480) sensu stricto specimens were used, from the 45 cm interval of unconsolidated sediments from the North Aegean Sea core M22-67 (245 m water depth; 38°21.87' N, 25°56.96' E) with a radiocarbon date (AMS ^{14}C) of 14.5 ka before present. The core consisted mainly of fine-grained hemipelagic muds and clays and represents a sedimentary archive of the last 85 kyr. The predominant clay minerals in the area are [30] and have been during the study interval [31] illite and smectite. The carbonate content of the sample was measured to be ~42% and since it was not from a sapropel or sapropelic layer its organic content is estimated to be less than 0.6% [32]. *G. ruber albus* s.s. was chosen for species under investigation because of its high abundance in the sample and its importance in paleoclimatic studies. It is likely that foraminiferal tests from different settings, and possibly different foraminifera species of different size, will respond differently to cleaning.

The sample was oven-dried overnight at 50 °C and was weighed unprocessed 24 g. Subsequently, it was divided into six aliquots (~4.10 g each) that were transferred into different 50 mL glass beakers and underwent treatment for 20 min at room temperature before wet sieving over a 63 μm mesh, using six processing methods: (1) addition of Calgon® (sodium hexametaphosphate, $(\text{NaPO}_3)_6$); (2) 2.5% hydrogen peroxide (H_2O_2); (3) 2.5% hydrogen peroxide and subsequent treatment with Calgon; (4) simultaneous treatment with 2.5% hydrogen peroxide and Calgon; (5) 4% hydrogen peroxide (H_2O_2); and (6) distilled water without chemical additions (see Table 1 for procedures). Hydrogen peroxide tends to acidify the solution by oxidizing the organic residuals, while Calgon is an alkaline dispersant

that neutralizes the charge of clay particles. Both reagents have traditionally been used in sediment or rock processing methods and in the present study they are applied in a specific order that aims to best use their effects.

Beaker 1 received treatment with Calgon by filling up the beaker with 5% Calgon solution (50 g $\text{Na}_6\text{P}_6\text{O}_{18}$ diluted in 950 mL distilled water) as proposed by [23]. Beaker 2 received treatment with 30% hydrogen peroxide by adding 4 mL of the reagent and filling up the beaker to 50 mL with distilled water, producing a 2.5% hydrogen peroxide solution. Beaker 3 received a “two step treatment”. The sample was initially treated with 2.5% hydrogen peroxide solution, like beaker 2, and after washed through a 63- μm sieve the remaining coarse fraction was transferred back to the beaker and treated with 5% Calgon solution, similar to beaker 1 (HyPerCal treatment). Beaker 4 received simultaneous treatment with hydrogen peroxide and Calgon by adding 4 mL of 30% hydrogen peroxide in 46 mL of 5% Calgon solution. Beaker 5 received treatment with 4% hydrogen peroxide solution by diluting 4 mL of 49.5% hydrogen peroxide in 46 mL distilled water, and beaker 6 only received treatment with distilled water. All beakers were gently agitated periodically sonicated every 2 min for 4 s, since a 4 s sonication step has been found to provide a greater detritus cleaning effect and minimize test breakage [23].

After their treatment the sample aliquots were thoroughly washed with tap water over a 63 μm wire mesh sieve and left overnight in the oven to dry at 50 °C. They were subsequently dry-sieved and the first random 15 non-fragmented *G. ruber albus* s.s. specimens from the 300–355 μm sieve fraction were picked from each aliquot for further analyses. In order to minimize the effect of specimen size (i.e., size of apertural openings, chamber size) in the cleaning efficiency tests from a narrow size fraction were used. This particular sieve fraction was chosen because of its frequent use in paleoceanographic studies. For assessing the effect that each treatment had on the surface ultrastructure of the foraminifera specimens, 5 specimens from each sample were mounted and gold-coated for SEM imaging. The samples were examined with a JEOL JSM-6390 instrument at a 1100 \times magnification, a working distance of 2.1 mm and an accelerating voltage of 20 kV in the Department of Geology and Geoscience of the National Kapodistrian University of Athens. In order to evaluate the extent of detritus removal from the interior of the specimens and quantify weight loss from each chemical treatment method, 5 additional specimens from each sample were weighed and subsequently scanned using X-ray computed tomography. The tests were initially weighed as a group of five individuals to obtain their average mass and subsequently in three groups of two individuals in order to record the weight variation in each sample. After weighing the tests were oriented and photographed (Figure 1) using a Leica M165 C stereo microscope with an integrated camera at the Department of Geology and Geoscience of the National Kapodistrian University of Athens. The weight analysis took place using a Sartorius microbalance (1 mg precision) also at the University of Athens.

The specimens were subsequently tomographically scanned using Synchrotron X-ray radiation at the Diamond Manchester Imaging Branchline (I13-2) at Diamond Light Source. The tests were transferred into quartz capillaries of 1 mm inner diameter (similar to [29]) that were subsequently attached to magnetic cryo-cap holders and mounted on to a goniometer. The data was acquired with partially coherent, pink X-ray beam which has broader energy spectrum centered around 27 keV. For each of the sessions exposure time of 0.5 s were used, at a 0.09 degree rotation step size producing an acquisition of 2000 projections with 2560 \times 2160 pixel resolution using a pco.edge 5.5 camera at a 4 \times magnification, which resulted in an effective pixel size of 0.8125 μm . The reconstruction of the acquisition data and their downsampling to 8bit tomographic images were performed with Savu package [33]. Links to the raw tomographic data are given the Appendix A below. The images were subsequently analyzed in Avizo software, where the test and sedimentary infilled areas were segmented and discriminated as described in Section 3.3 of [24].

Table 1. Table summarizing the different cleaning methods followed.

Method	Method Name	Chemical Treatment			Treatment Time	Processing	
		Step 1	Step 2	Step 3		Step 4	Step 5
1	“Calgon”	50 mL Calgon 5%	-	-	20 min sonicated every 2 min for 4 s	Wet sieving over >63 µm mesh	Dried overnight
2	“30% Peroxide”	2.5% hydrogen peroxide (4 mL of H ₂ O ₂ were added to 46 mL distilled water)	-	-	20 min sonicated every 2 min for 4 s	Wet sieving over >63 µm mesh	Dried overnight
3	“HyPerCal treatment”	4 mL of 30% H ₂ O ₂ added to 46 mL distilled water (2.5% hydrogen peroxide)	Wet sieving over >63 µm mesh	4 mL 5% Calgon were added in 46 mL distilled water	20 + 20 min sonicated every 2 min for 4 s	Wet sieving over >63 µm mesh	Dried overnight
4	“Mixed Calgon and peroxide”	4 mL of 30% H ₂ O ₂ added in 46 mL of 5% Calgon solution	-	-	20 min sonicated every 2 min for 4 s	Wet sieving over >63 µm mesh	Dried overnight
5	“4% Peroxide”	4 mL of 49.5% H ₂ O ₂ added to 46 mL distilled water (4% hydrogen peroxide)	-	-	20 min sonicated every 2 min for 4 s	Wet sieving over >63 µm mesh	Dried overnight
6	“Control”	Treatment only with distilled water	-	-	20 min sonicated every 2 min for 4 s	Wet sieving over >63 µm mesh	Dried overnight

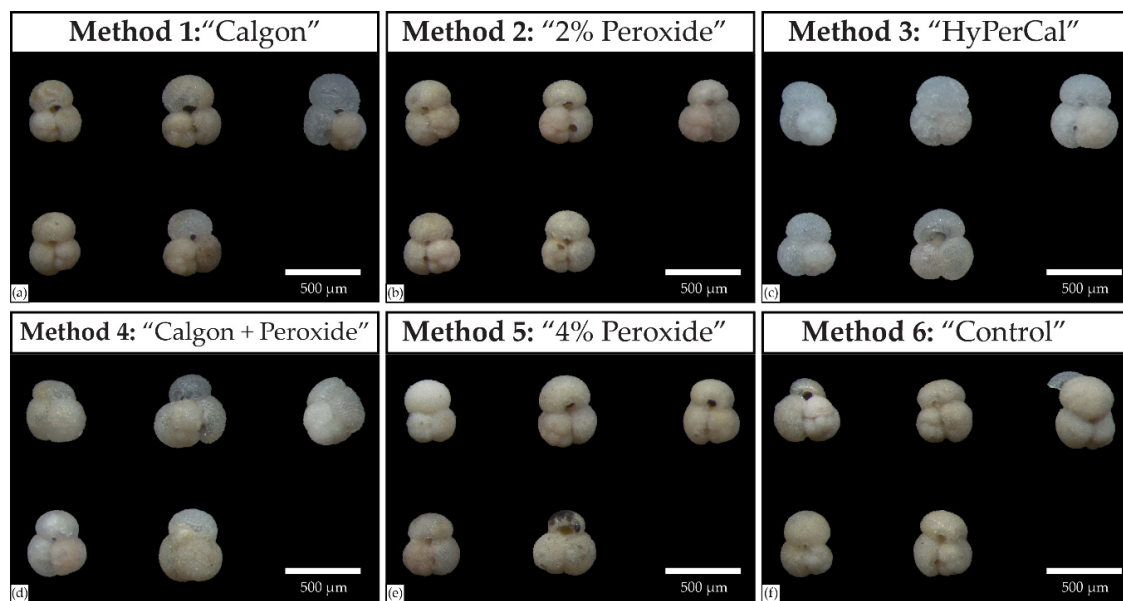


Figure 1. Images of the analyzed specimens after their treatment with the different cleaning protocols.

3. Results

There are some general observations of the behavior of the different sample solutions that deserve to be noted here. Due to the cohesion degree of the core sample not all treatment solutions were capable to completely disintegrate the sample's mass. The most effective reagent to turn the sample solution into homogeneous mud slurry was H_2O_2 regardless of its concentration or admixture. The sample aliquots that were treated with water or $\text{Na}_6\text{O}_{18}\text{P}_6$ solution did not completely disintegrate and small chunks of sediment were left still standing in the beaker that required some extra mechanical effort to dissolve better. Finally, beaker 4 which contained simultaneously both H_2O_2 and $\text{Na}_6\text{O}_{18}\text{P}_6$ exhibited strong foaming during treatment time.

3.1. Scanning Electron Microscopic Analysis

The results of the SEM analysis are shown in Figure 2. It can be seen that the surface ultrastructure of the tests that underwent HyPerCal treatment, initially with H_2O_2 and subsequently with $\text{Na}_6\text{O}_{18}\text{P}_6$, is almost completely free from detrital particles and clay impurities (Figure 2k–o). This treatment method removed detritus from all the different ultrastructural test features such as pores, ridges, interpore area and spine bases, even in the case of dissolved and etched interpore surfaces (Figure 2n). The treatment with H_2O_2 of diverse concentrations (Methods 2 and 5) showed that the different ultrastructural features of all the specimens were covered to some degree with detritus. Treatment with $\text{Na}_6\text{O}_{18}\text{P}_6$ or water had some better cleaning effects especially for some of the specimens (Figure 2a–e,z–ad) and the same is true for Method 4, of simultaneous treatment with hydrogen H_2O_2 and $\text{Na}_6\text{O}_{18}\text{P}_6$.

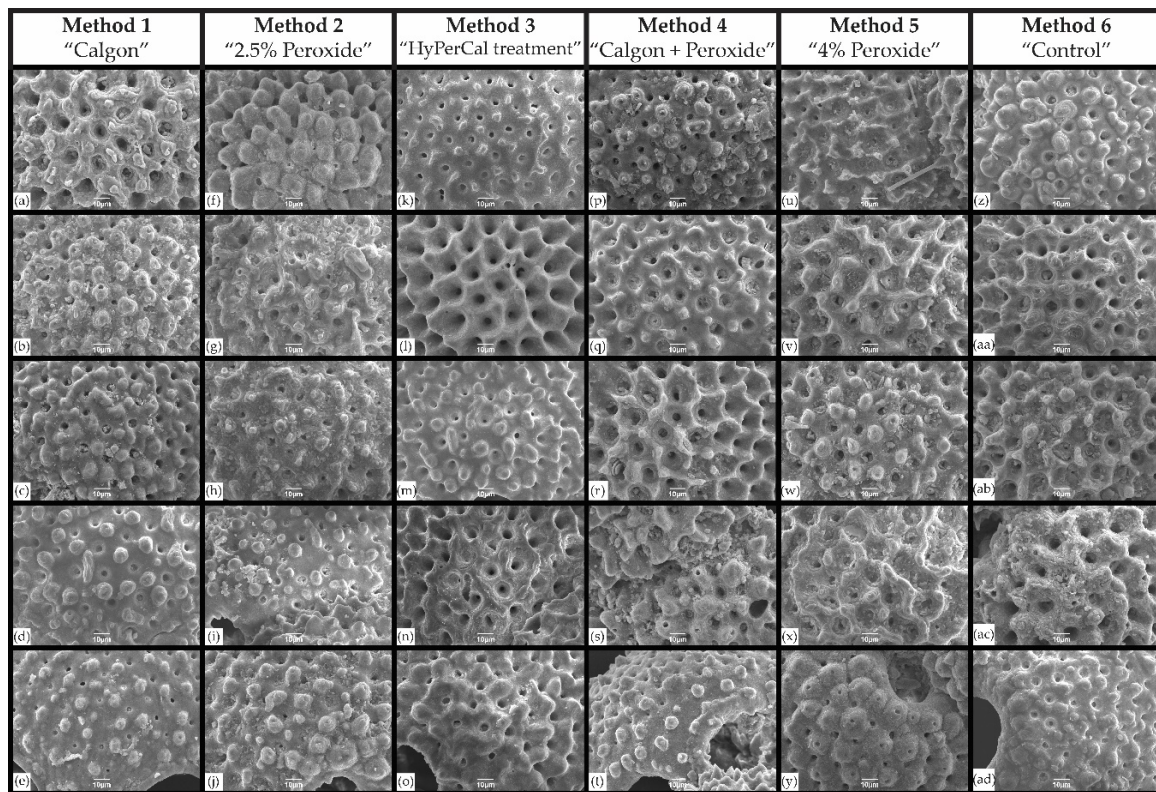


Figure 2. Scanning electron microscope images of the ultrastructure of the specimens after their treatment with the different cleaning methods: (a–e) tomographs of specimens after treatment with $\text{Na}_6\text{O}_{18}\text{P}_6$, (f–j) images of specimens after treatment with 2.5% H_2O_2 solution; (k–o) images after treatment first with 2.5% H_2O_2 and subsequently with $\text{Na}_6\text{O}_{18}\text{P}_6$ solution (HyPerCal); (p–t) images after treatment simultaneously with 2.5% H_2O_2 and $\text{Na}_6\text{O}_{18}\text{P}_6$ solution; (u–y) images after treatment with 4% H_2O_2 , and (z–ad) images after treatment with only with distilled water.

3.2. Synchrotron X-ray Absorption and Weight Analysis

Tomographic slices of the scanned specimens that underwent different treatment are shown in Figure 3 and the results of the tomographic analysis together with the weight measurements are summarized in Table 2. The visual inspection of the tomographs clearly shows that the HyPerCal treatment of Method 3 is the most effective way to eliminate contamination from the internal tests cavities of foraminifera. As it can be seen in Figure 3k–o even the smallest chambers or the secondary apertures and pores are free from detrital material. The two-step treatment with H_2O_2 and subsequently with $\text{Na}_6\text{O}_{18}\text{P}_6$ shows also reduced contamination in the smaller chambers but there is still sedimentary material attached to the interior of the larger chamber walls. $\text{Na}_6\text{O}_{18}\text{P}_6$ alone is less effective in removing contamination, especially in the smaller chambers, while treatment only with water leaves the test infilling in an aggregated form. Treatment with H_2O_2 has left the tests with considerable amounts of detritus and the cohesion of this remaining detrital mass seems to increase with H_2O_2 concentration.

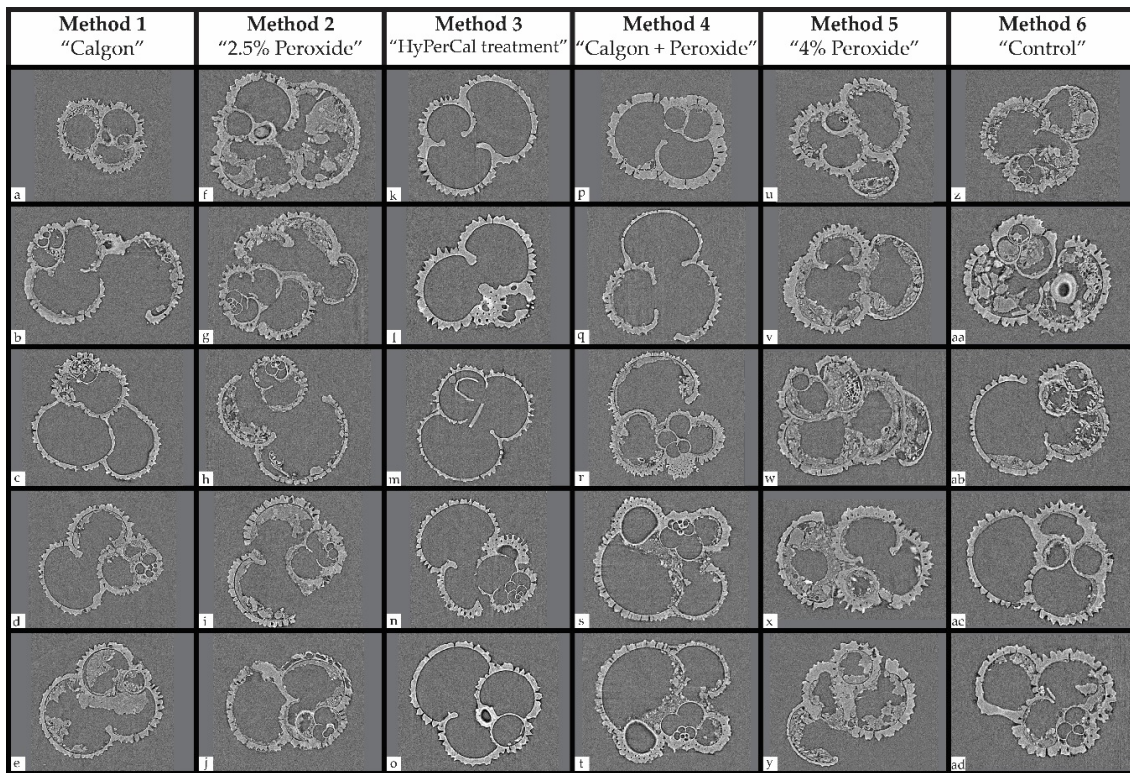


Figure 3. X-ray tomographic images of the interior of the specimens after their treatment with the different cleaning methods: (a–e) tomographs of specimens after treatment with $\text{Na}_6\text{O}_{18}\text{P}_6$, (f–j) tomographs of specimens after treatment with 2.5% H_2O_2 solution, (k–o) tomographs after treatment first with 2.5% H_2O_2 and subsequently with $\text{Na}_6\text{O}_{18}\text{P}_6$ solution (HyPerCal), (p–t) tomographs after treatment simultaneously with 2.5% H_2O_2 and $\text{Na}_6\text{O}_{18}\text{P}_6$ solution, (u–y) tomographs after treatment with 4% H_2O_2 , and (z–ad) tomographs after treatment with only with distilled water.

Table 2. Table showing the results of the X-ray tomographic and weight analyses. The degree of contamination is given as a percentage of cell's volume. Furthermore, the difference in the measured weights in regard to the average shell weight of the least contaminated tests.

Method	Method Name	Nº of Tests	Contamination (%)	Weight (μg)	Weight Diff.
1	"Calgon"	5	14 (± 12)	23.8 (± 1.6)	21%
2	"2.5% Peroxide"	5	18 (± 6)	28.2 (± 2.8)	44%
3	"PerCal treatment"	5	0 (± 1)	19.6 (± 1.4)	-
4	"Mixed Calgon and peroxide"	5	5 (± 5)	22.0 (± 2.0)	12%
5	"4% Peroxide"	5	21 (± 6)	24.4 (± 0.9)	25%
6	"Control"	5	12 (± 6)	26.4 (± 3.8)	35%

Apart from the visual inspection, the X-ray analysis allowed the determination of the total foraminifera cell volume and that of the area in the interior of the test, which is occupied by sedimentary infill. Thus the degree of contamination of each test is presented in Table 2 as the percentage of detritus within the cell's volume. It can be seen that the HyPerCal treatment of the sample with H_2O_2 and $\text{Na}_6\text{O}_{18}\text{P}_6$ in two steps has almost completely removed the sediment infill (0%, Table 2) from the test's interior, as this is also evident in Figure 3k–o. The simultaneous treatment with H_2O_2 and $\text{Na}_6\text{O}_{18}\text{P}_6$ within the same solution had adequate results since detrital contamination was reduced to only 5% by volume. Treatment with $\text{Na}_6\text{O}_{18}\text{P}_6$ or water had a similar effect on detrital removal by reducing

contamination to 14% and 12% respectively, while treatment with H_2O_2 (of different concentrations) had the minimum efficiency in specimen cleaning.

Shell weight is found to be a function of the degree of contamination as shown in Figure 4. It can be seen that samples treated with hydrogen peroxide solution group in the right corner of the graph, while samples treated with aqueous solutions (i.e., water or Calgon) group in its middle. The heaviest tests were the ones that were treated with 2.5% hydrogen peroxide (Method 2). Their average shell weight was 44% greater than that measured for the least contaminated tests. Although treatment with 4% hydrogen peroxide produced consistently lower shell weights its effect on contamination removal was the lowest, suggesting possibly calcite dissolution by the unbuffered solution [34]. Treatment with water produced weights increased by 35% compared to the actual/uncontaminated ones. From the single-constituent solutions Calgon was the one to have the greatest effect on shell weight but also with the greatest variability (12%) in the extent of sediment detrital removal. The simultaneous treatment of the sample with Calgon and hydrogen peroxide is found to be an effective method for specimen cleaning since contamination was found consistently reduced to 5%. Finally, the most effective method that almost completely removed contamination ($0\% \pm 1\%$) was the HyPerCal treatment.

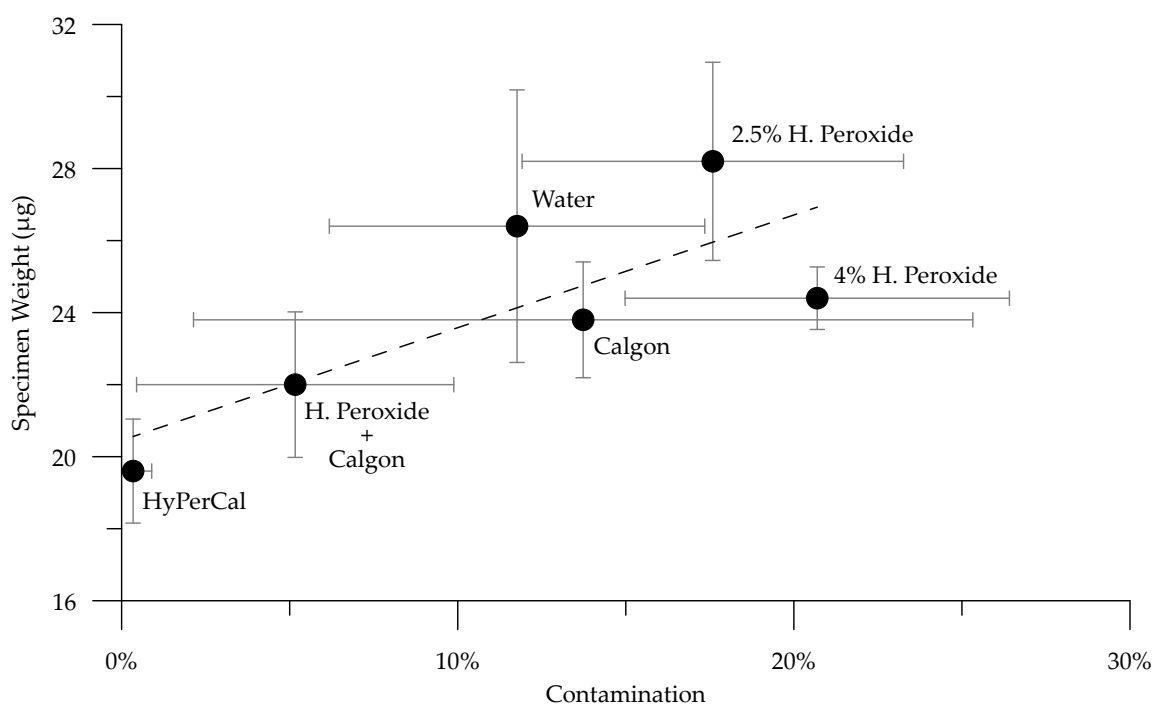


Figure 4. Plot of *G. ruber albus* s.s. shell weights after treatment with the different cleaning methods against their contamination as per volume percentage.

4. Discussion

We performed a systematic experiment with chemical treatments commonly utilized to disaggregate marine sediment and which are known to not significantly affect foraminiferal based proxies, such as species abundance, shell fragmentation, $\delta^{18}\text{O}$, $\delta^{13}\text{C}$, and Mg/Ca . The chemical agents used in solutions were hydrogen peroxide (H_2O_2) in two different concentrations, 5% Calgon (sodium hexametaphosphate, $\text{Na}_6\text{P}_6\text{O}_{18}$), a swap and a combination of them. We find that the most effective way for preparing foraminifera samples for their subsequent micropaleontological or geochemical analyses is the initial cleaning of the sedimentary material with H_2O_2 followed by treatment of the sieved sample residual with $\text{Na}_6\text{O}_{18}\text{P}_6$ solution and we refer to this procedure as HyPerCal. In the present experiment the samples were treated for 20 min in every solution and were sonicated every 2 min for 4 s in order to minimize shell breakage [23] but duration of treatment may

vary depending on the cohesion of the sedimentary mass. After cleaning, single-species specimens from a certain sieve fraction were picked, weighed, and subsequently inspected using light microscope, SEM and S μ CT. The analyses showed that the different procedures had a variable effect in contamination removal (Figure 4) from the surface and the interior of the examined specimens and that the HyPerCal treatment left the specimens free of (surface or internal) sedimentary residuals, shiny and translucent (Figure 1c).

Sodium hexametaphosphate is a common dispersing agent in research of marine sediments and is more effective than water in removing clay clumps from tests interiors [35], while foraminifera shell weight loss has been previously reported with [21] and without [23] the use of it during cleaning. Our tomographic analysis supports previous studies and confirms that weight differences are the result of sediment contamination removal. The initial treatment with H₂O₂ promotes the degradation of organic matter, which is the major binding agent in benthic sediments [36] and thus minimizing the adhesive forces within the medium. Cohesive forces are at molecular scale the result of the attractive interactions in vacuum between contiguous particles of the same medium, while the adhesive forces are defined as the additional binding forces between particles, due to the presence of a second, interparticle medium [37]. The dispersing action of Na₆O₁₈P₆, as a second treatment step, helps to neutralize the attraction electrostatic forces between (clay) particles [38] and is thus reducing particle cohesion. The use of only one of these two reagents alone (Na₆O₁₈P₆, H₂O₂) in specimen cleaning did not produce satisfying results both under the SEM and S μ CT analyses. The use of both reagents in the same solution, compared to HyPerCal, produced fairly satisfactory results by reducing contamination to only 5%. The high efficiency, however, of the HyPerCal treatment can also stem from the fact that during a two-step treatment the sample processed and sonicated twice as much or from the fact that Na₆O₁₈P₆ is only applied on the coarse fraction of sample, free of a substantial amount of material.

Due to the highly reactive nature of the used reagents, there is number of studies that accuse them for foraminifera specimen dissolution [21,34,39]. The release of CO₂ during organic matter oxidation by the unbuffered H₂O₂ increases ambient pH and raises dissolution concerns, while Na₆O₁₈P₆ is known to react with calcite [40]. Nevertheless, both of our imaging analyses do not reveal signs of foraminifera calcite dissolution. Dissolution can be assessed by the preservation state of four ultrastructural test features such as pores, interpore space, spines, and ridges [25]. As dissolution proceeds, pores get widened, the interpore areas is etched, ridges and spines become denuded. However, such features are not observed on the well decontaminated ultrastructural surface of most of the tests that were cleaned with HyPerCal (Figure 2k–o) that have thus undergone treatment with both reagents. Further evidence of negligible dissolution can be found by the examination of the S μ C-tomographs that show intact chamber walls and well defined initial juvenile chambers (Figure 3k–o), since dissolution first attacks the high-Mg calcite parts of the test. The first signs of dissolution apparent in CT images is that chamber walls become blurred and paler in color, especially in the middle, while the smallest inner chambers start to vanish [41]. Such alterations are not here observed possibly also due to the low organic content of the oligotrophic in nature Mediterranean Sea.

The effectiveness of sediment cleaning procedures is a function sediment matrix mineralogy, grain size and degree of consolidation. The present sediment core material consists of fine-grained (hemipelagic) sediment and originates from the Southeastern Mediterranean basin, which is known for the fine particle size of its clay minerals [42]. The chemical treatment tested here has proved appropriate for removal of the fine material that are usually found in sedimentary basins and should remain so for recent sediment, where the depth of burial is not considered important to initiate diagenetic alteration of the clay minerals [43]. The efficiency of the HyPerCal procedure in the cleaning of calcitic microfossils makes it complementary for foraminifera shell weight studies since it was shown to bring the measured weight closer to that of an “original” shell. Furthermore, it paves the way for its use in modern analytical techniques that require some degree of automatization, such as image recognition software that are unable to recognize a lot of foraminifera images, whose umbilical aperture is not fully cleaned and is infilled with remaining nannofossil ooze [28]. On the other hand, it has proved

beneficial for the upcoming practice of microfossil X-ray tomography, since CT image analysis software cannot easily discriminate between contaminated areas and areas referring to the foraminifera tests unless (subjective) manual labor intensive segmentation is employed [24].

5. Conclusions

In the present study a sediment core sample of late Quaternary age was divided in six aliquots each of which was treated with reagents that do not alter foraminifera calcite geochemistry following different cleaning procedures and the efficiency of each method in specimen cleaning was assessed using SEM and X-ray tomography. The results of the visualization analyses were combined with shell weight measurements and allowed us to conclude that the method that has proven the most effective in removing fine detritus trapped within foraminiferal tests is a two-step treatment of the sedimentary material, named here HyPerCal treatment, initially with 2.5% hydrogen peroxide and subsequently with 5% Calgon solutions. The proposed protocol minimizes discrepancies in foraminifera shell weight measurements and greatly facilitates microfossil X-ray imaging analyses.

Author Contributions: Conceptualization, S.D.Z.; original draft preparation, G.K. and S.D.Z.; laboratory analyses, G.G., S.D.Z. and P.M.; SEM data acquisition, E.B. and V.L.; synchrotron data acquisition, V.S.C.K. and S.M., synchrotron data scientific computing and analysis, K.W. and S.D.Z.; writing—review and editing, G.K., S.D.Z. and A.A.; supervision, A.A. All authors have read and agreed to the published version of the manuscript.

Funding: This research received no external funding.

Acknowledgments: We would like to acknowledge Efterpi Koskeridou and Danae Thivaïou for access to the camera light stereomicroscope and photograph acquisition. This synchrotron X-ray scanning work was carried out with the support of Diamond Light Source, instrument I13-2 (part of proposal MG23868).

Conflicts of Interest: The authors declare no conflict of interest.

Appendix A

The S μ CT reconstructed data of (individual) specimens that were cleaned with the different cleaning methods are available online at: (1) <https://doi.org/10.6084/m9.figshare.13333772> for those treated with 5% Na₆P₆O₁₈, (2) <https://doi.org/10.6084/m9.figshare.13335002> for those treated with 2.5% H₂O₂, (3) <https://doi.org/10.6084/m9.figshare.13335833> for those that underwent HyPerCal treatment, (4) <https://doi.org/10.6084/m9.figshare.13335890> for those that treated simultaneously with 2.5% H₂O₂ and 5% Na₆P₆O₁₈, (5) <https://doi.org/10.6084/m9.figshare.13335908> for those treated with 4% H₂O₂, and (6) <https://doi.org/10.6084/m9.figshare.13335935> for those treated only with distilled water.

References

1. Kucera, M. Planktonic Foraminifera as Tracers of Past Oceanic Environments. In *Developments in Marine Geology*; Hillaire-Marcel, C., De Vernal, A., Eds.; Elsevier: Amsterdam, The Netherlands, 2007; Volume 1, pp. 213–262.
2. Shackleton, N.J. Oxygen isotopes, ice volume and sea level. *Quat. Sci. Rev.* **1987**, *6*, 183–190. [CrossRef]
3. Emiliani, C. Depth habitats of some species of pelagic foraminifera as indicated by oxygen isotope ratios. *Am. J. Sci.* **1954**, *252*, 149–158. [CrossRef]
4. Anand, P.; Elderfield, H.; Conte, M.H. Calibration of Mg/Ca thermometry in planktonic foraminifera from a sediment trap time series. *Paleoceanography* **2003**, *18*, 1050. [CrossRef]
5. Brown, S.J.; Elderfield, H. Variations in Mg/Ca and Sr/Ca ratios of planktonic foraminifera caused by postdepositional dissolution: Evidence of shallow Mg-dependent dissolution. *Paleoceanography* **1996**, *11*, 543–551. [CrossRef]
6. Hönisch, B.; Hemming, N.G. Surface ocean pH response to variations in pCO₂ through two full glacial cycles. *Earth Planet. Sci. Lett.* **2005**, *236*, 305–314. [CrossRef]
7. Berger, W.H. Planktonic Foraminifera: Selective solution and the lysocline. *Mar. Geol.* **1970**, *8*, 111–138. [CrossRef]

8. Kucera, M.; Weinelt, M.; Kiefer, T.; Pflaumann, U.; Hayes, A.; Weinelt, M.; Chen, M.-T.; Mix, A.C.; Barrows, T.T.; Cortijo, E.; et al. Reconstruction of sea-surface temperatures from assemblages of planktonic foraminifera: Multi-technique approach based on geographically constrained calibration data sets and its application to glacial Atlantic and Pacific Oceans. *Quat. Sci. Rev.* **2005**, *24*, 951–998. [[CrossRef](#)]
9. Antonarakou, A.; Kontakiotis, G.; Karageorgis, A.P.; Besiou, E.; Zarkogiannis, S.; Drinia, H.; Mortyn, G.P.; Tripsanas, E. Eco-biostratigraphic advances on late Quaternary geochronology and palaeoclimate: The marginal Gulf of Mexico analogue. *Geol. Q.* **2019**, *63*, 178–191. [[CrossRef](#)]
10. Speijer, R.P.; Van Loo, D.; Masschaele, B.; Vlassenbroeck, J.; Cnudde, V.; Jacobs, P. Quantifying foraminiferal growth with high-resolution X-ray computed tomography: New opportunities in foraminiferal ontogeny, phylogeny, and paleoceanographic applications. *Geosphere* **2008**, *4*, 760–763. [[CrossRef](#)]
11. Zarkogiannis, S.; Kontakiotis, G.; Antonarakou, A. Logarithmic expression of *Globigerina bulloides* shell evolution through the biometric analysis: Paleoceanographic implications for the late Quaternary. *IOP Conf. Ser. Earth Environ. Sci.* **2019**, *362*, 012100. [[CrossRef](#)]
12. Caromel, A.G.M.; Schmidt, D.N.; Phillips, J.C.; Rayfield, E.J. Hydrodynamic constraints on the evolution and ecology of planktic foraminifera. *Mar. Micropaleontol.* **2014**, *106*, 69–78. [[CrossRef](#)]
13. Schmidt, D.N.; Thierstein, H.R.; Bollmann, J.; Schiebel, R. Abiotic forcing of plankton evolution in the Cenozoic. *Science* **2004**, *303*, 207–210. [[CrossRef](#)] [[PubMed](#)]
14. Zarkogiannis, S.; Kontakiotis, G.; Antonarakou, A. Recent planktonic foraminifera population and size response to Eastern Mediterranean hydrography. *Rev. Micropaléontologie* **2020**, *69*, 100450. [[CrossRef](#)]
15. Barker, S.; Elderfield, H. Foraminiferal calcification response to glacial-interglacial changes in atmospheric CO₂. *Science* **2002**, *297*, 833–836. [[CrossRef](#)]
16. Zarkogiannis, S.D.; Antonarakou, A.; Tripathi, A.; Kontakiotis, G.; Mortyn, P.G.; Drinia, H.; Greaves, M. Influence of surface ocean density on planktonic foraminifera calcification. *Sci. Rep.* **2019**, *9*, 533. [[CrossRef](#)]
17. Lohmann, G.P. A model for variation in the chemistry of planktonic foraminifera due to secondary calcification and selective dissolution. *Paleoceanography* **1995**, *10*, 445–457. [[CrossRef](#)]
18. Broecker, W.; Clark, E. An evaluation of Lohmann's Foraminifera weight dissolution index. *Paleoceanography* **2001**, *16*, 531–534. [[CrossRef](#)]
19. Vetter, L.; Spero, H.J.; Russell, A.D.; Fehrenbacher, J.S. LA-ICP-MS depth profiling perspective on cleaning protocols for elemental analyses in planktic foraminifers. *Geochem. Geophys. Geosyst.* **2013**, *14*, 2916–2931. [[CrossRef](#)]
20. Barker, S.; Greaves, M.; Elderfield, H. A study of cleaning procedures used for foraminiferal Mg/Ca paleothermometry. *Geochem. Geophys. Geosyst.* **2003**, *4*, 8407. [[CrossRef](#)]
21. Feldmeijer, W.; Metcalfe, B.; Scussolini, P.; Arthur, K. The effect of chemical pretreatment of sediment upon foraminiferal-based proxies. *Geochem. Geophys. Geosyst.* **2013**, *14*, 3996–4014. [[CrossRef](#)]
22. Rosenthal, Y.; Perron-Cashman, S.; Lear, C.H.; Bard, E.; Barker, S.; Billups, K.; Bryan, M.; Delaney, M.L.; deMenocal, P.B.; Dwyer, G.S.; et al. Interlaboratory comparison study of Mg/Ca and Sr/Ca measurements in planktonic foraminifera for paleoceanographic research. *Geochem. Geophys. Geosyst.* **2004**, *5*, Q04D09. [[CrossRef](#)]
23. Qin, B.; Li, T.; Chang, F.; Xiong, Z.; Algeo, T.J. An Improved Protocol For Cleaning of Planktonic Foraminifera For Shell Weight Measurement. *J. Sediment. Res.* **2016**, *86*, 431–437. [[CrossRef](#)]
24. Zarkogiannis, S.D.; Antonarakou, A.; Fernandez, V.; Mortyn, P.G.; Kontakiotis, G.; Drinia, H.; Greaves, M. Evidence of stable foraminifera biomineralization during the last two climate cycles in the tropical Atlantic Ocean. *J. Mar. Sci. Eng.* **2020**, *8*, 737. [[CrossRef](#)]
25. Volbers, A.N.A.; Henrich, R. Late Quaternary variations in calcium carbonate preservation of deep-sea sediments in the northern Cape Basin: Results from a multiproxy approach. *Mar. Geol.* **2002**, *180*, 203–220. [[CrossRef](#)]
26. Weinkauf, M.F.G.; Zwick, M.M.; Kučera, M. Constraining the Role of Shell Porosity in the Regulation of Shell Calcification Intensity in the Modern Planktonic Foraminifer *Orbulina Universa* d'Orbigny. *J. Foraminifer. Res.* **2020**, *50*, 195–203. [[CrossRef](#)]
27. Hsiang, A.Y.; Brombacher, A.; Rillo, M.C.; Mleneck-Vautravers, M.J.; Conn, S.; Lordsmith, S.; Jentzen, A.; Henehan, M.J.; Metcalfe, B.; Fenton, I.S.; et al. Endless Forams: >34,000 Modern Planktonic Foraminiferal Images for Taxonomic Training and Automated Species Recognition Using Convolutional Neural Networks. *Paleoceanogr. Paleoclimatol.* **2019**, *34*, 1157–1177. [[CrossRef](#)]

28. Marchant, R.; Tetard, M.; Pratiwi, A.; Adebayo, M.; de Garidel-Thoron, T. Automated analysis of foraminifera fossil records by image classification using a convolutional neural network. *J. Micropalaeontol.* **2020**, *39*, 183–202. [\[CrossRef\]](#)
29. Zarkogiannis, S.; Fernandez, V.; Greaves, M.; Mortyn, P.G.; Kontakiotis, G.; Antonarakou, A. X-ray tomographic data of planktonic foraminifera species *Globigerina bulloides* from the Eastern Tropical Atlantic across Termination II. *Gigabyte* **2020**, *1*, 1–10. [\[CrossRef\]](#)
30. Ehrmann, W.; Schmiedl, G.; Hamann, Y.; Kuhnt, T. Distribution of clay minerals in surface sediments of the Aegean Sea: A compilation. *Int. J. Earth Sci.* **2006**, *96*, 769. [\[CrossRef\]](#)
31. Ehrmann, W.; Schmiedl, G.; Hamann, Y.; Kuhnt, T.; Hemleben, C.; Siebel, W. Clay minerals in late glacial and Holocene sediments of the northern and southern Aegean Sea. *Palaeogeogr. Palaeoclimatol. Palaeoecol.* **2007**, *249*, 36–57. [\[CrossRef\]](#)
32. Kidd, R.B.; Cita, M.B.; Ryan, W.B.F. Stratigraphy of eastern Mediterranean sapropel sequences recovered during DSDP Leg 42A and their paleoenvironmental significance. In *Initial Reports of the Deep Sea Drilling Project/1975/Malaga*; Government Printing Office: Washington, DC, USA, 1978; pp. 421–443.
33. Atwood, R.C.; Bodey, A.J.; Price, S.W.T.; Basham, M.; Drakopoulos, M. A high-throughput system for high-quality tomographic reconstruction of large datasets at Diamond Light Source. *Philos. Trans. R. Soc. A Math. Phys. Eng. Sci.* **2015**, *373*, 20140398. [\[CrossRef\]](#) [\[PubMed\]](#)
34. D'Onofrio, R.; Luciani, V. Do different extraction techniques impact planktic foraminiferal assemblages? An early Eocene case study. *Mar. Micropaleontol.* **2020**, *155*, 101795. [\[CrossRef\]](#)
35. Kilmer, V.J.; Alexander, L.T. Methods of making mechanical analyses of soils. *Soil Sci.* **1949**, *68*, 15–24. [\[CrossRef\]](#)
36. Righetti, M.; Lucarelli, C. May the Shields theory be extended to cohesive and adhesive benthic sediments? *J. Geophys. Res. Ocean.* **2007**, *112*, C05039. [\[CrossRef\]](#)
37. Israelachvili, J.N. *Intermolecular and Surface Forces*; Academic Press: San Diego, CA, USA, 2011; p. 674. [\[CrossRef\]](#)
38. Castellini, E.; Lusvardi, G.; Malavasi, G.; Menabue, L. Thermodynamic aspects of the adsorption of hexametaphosphate on kaolinite. *J. Colloid Interface Sci.* **2005**, *292*, 322–329. [\[CrossRef\]](#)
39. Green, O.R. Extraction Techniques for Calcareous Microfossils from Argillaceous Sediments. In *A Manual of Practical Laboratory and Field Techniques in Palaeobiology*; Springer: Dordrecht, The Netherlands, 2001; pp. 334–341. [\[CrossRef\]](#)
40. Thomson, R.T. Some properties of sodium hexametaphosphate. *Analyst* **1936**, *61*, 320–323. [\[CrossRef\]](#)
41. Johnstone, H.J.H.; Schulz, M.; Barker, S.; Elderfield, H. Inside story: An X-ray computed tomography method for assessing dissolution in the tests of planktonic foraminifera. *Mar. Micropaleontol.* **2010**, *77*, 58–70. [\[CrossRef\]](#)
42. Weir, A.H.; Ormerod, E.C.; El Mansey, I.M.I. Clay mineralogy of sediments of the western Nile Delta. *Clay Miner.* **2018**, *10*, 369–386. [\[CrossRef\]](#)
43. Rostási, Á.; Raucsik, B.; Varga, A. Palaeoenvironmental controls on the clay mineralogy of Carnian sections from the Transdanubian Range (Hungary). *Palaeogeogr. Palaeoclimatol. Palaeoecol.* **2011**, *300*, 101–112. [\[CrossRef\]](#)

Publisher's Note: MDPI stays neutral with regard to jurisdictional claims in published maps and institutional affiliations.



© 2020 by the authors. Licensee MDPI, Basel, Switzerland. This article is an open access article distributed under the terms and conditions of the Creative Commons Attribution (CC BY) license (<http://creativecommons.org/licenses/by/4.0/>).